

## Supplementary Material

### Excellent energy storage and discharge performances in $\text{Na}_{1/2}\text{Bi}_{1/2}\text{TiO}_3$ -based ergodic relaxors by enlarging $[\text{AO}_{12}]$ cages

Miaomiao Li, Mankang Zhu, Mupeng Zheng, Yudong Hou, Jitong Wang, Xiaolian Chao,  
Zupei Yang, Jinling Zhou, Ke Wang, Xiaoxing Ke

#### Sample thickness control

Considering the electric breakdown limitation and measuring requirement, the dimensions of samples for different ferroelectric measurements is listed in Table S1.

Table S1. Dimensions of samples for ferroelectric measurement

Diagram Sample size	Fig. 3 and 4(a)	Fig. 4(c)	Fig. 5(a)	Fig. 8(a-d)	Fig. 9(a-b)
Thickness (mm)	0.40-0.50	0.16	0.11	0.15	0.12
Area (mm <sup>2</sup> )	75.60-76.50	12.56	0.29	0.29	3.14

#### Cell Parameter Determination

The cell parameter is determined by a software MDI Jade (Materials Data, Inc., Livermore, California) based on the XRD patterns. Fig. S1 gives the typical Refinement Result of unpoled NBT-7BT sample. As shown in Fig. S1, the unpoled NBT-7BT ceramic presents a cubic structure, and its cell volume  $V_0$  is 59.51 Å<sup>3</sup>, similar to that in previous report<sup>1,2</sup>. The cell parameter of KBZN100x sample are obtained in same way. Table S2 gives the cell volume  $V$  of sample KBZN100x and the difference  $V-V_0$ . And the composition dependence of  $V-V_0$  is presented in Fig. 2.

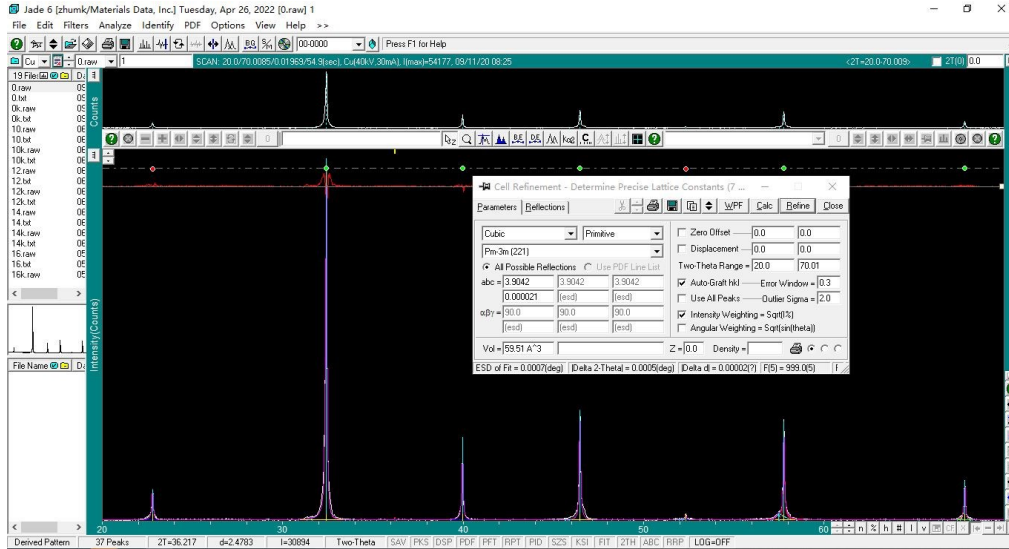


Fig. S1. Screenshot of the cell refinement of MDI Jade software for NBT-7BT sample

Table S2 The result of cell refinement of KBZN100x samples by MDI Jade

Sample	Axis length $a$ (Å)	Cell volume $V$ (Å <sup>3</sup> )	$V-V_0$ (Å <sup>3</sup> )
$x=0$	3.9042	59.51	0
$x=0.10$	3.9099	59.77	0.26
$x=0.12$	3.9119	59.86	0.35
$x=0.14$	3.9147	59.99	0.48
$x=0.16$	3.9169	60.09	0.58

## Density Measurement

The apparent density ( $\rho$ ) of bulk ceramic was measured by Archimedes repulsion method using a precision balance (Mettler-Toledo XS104, Switzerland) with a density kit. By measuring the weight of a ceramic sample in air and water, the apparent density is calculated as follows:

$$\rho = \frac{\rho_0 m_1}{m_1 - m_2} \quad (1)$$

Where,  $\rho_0$  is the density of water,  $m_1$  and  $m_2$  are the mass of the samples in air and water respectively. The theoretical density ( $\rho_t$ ) is determined according to the cell

parameters obtained by X-ray diffraction, the calculation formula as follows:

$$\rho_t = \frac{M}{V_{\text{cell}}} \quad (2)$$

where,  $M$  is the molecular weight,  $V_{\text{cell}}$  is the cell volume.

According to the measured and theoretical density, the relative density ( $\rho_r$ ) of the sample can be determined:

$$\rho_r = \frac{\rho}{\rho_t} \times 100\% \quad (3)$$

Table S3 lists the apparent density and relative density of KBZN100x samples. As shown in Table S3, all samples present a high relative density over 95%, reflecting the well sintering ability. With the introduction of KBZN, the relative density  $\rho_r$  decreases gradually. This may be related to the increase of theoretical density due to the large molecular weight of KBZN than that of NBT-7BT and the volatilization of K/Bi caused due the increase of K/Bi content.

Table S3 The apparent density and relative density of KBZN100x samples

Samples	$\rho$ (g/cm <sup>3</sup> )	$\rho_t$ (g/cm <sup>3</sup> )	$\rho_r$ (%)
KBZN10	5.81	6.03	96.2
KBZN12	5.80	6.04	95.9
KBZN14	5.79	6.06	95.5
KBZN16	5.78	6.09	95.0

## Micromorphology and Grain Size Distribution

The micromorphology was observed using a scanning electron microscope (SEM, S-3500N, Hitachi, Tokyo, Japan) on the polished and thermally-etched fractured surface. Fig. S2 gives the SEM pictures of samples KBZN100x. As shown in Fig. S2, a dense and uniform microstructure of KBZN100x. Besides, the grain size distribution was analyzed based on the grains over 100. The average grain size  $D$  and the error are determined statistically by more than 100 grains.

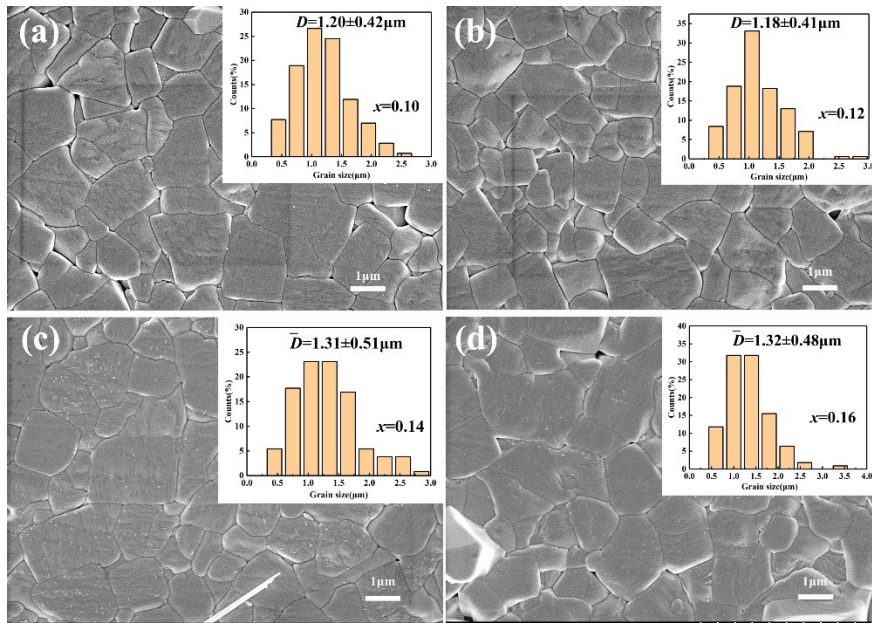


Fig. S2. SEM micrographs of KBZN100 $x$  samples: (a)  $x = 0.10$ , (b)  $x = 0.12$ , (c)  $x = 0.14$  and (d)  $x = 0.16$ . The insets shows the statistics on the grain size, which shows a average grain size about 1.2~ 1.3  $\mu\text{m}$ .

### Temperature-Dependent Dielectric Responses of NBT-7BT ceramics

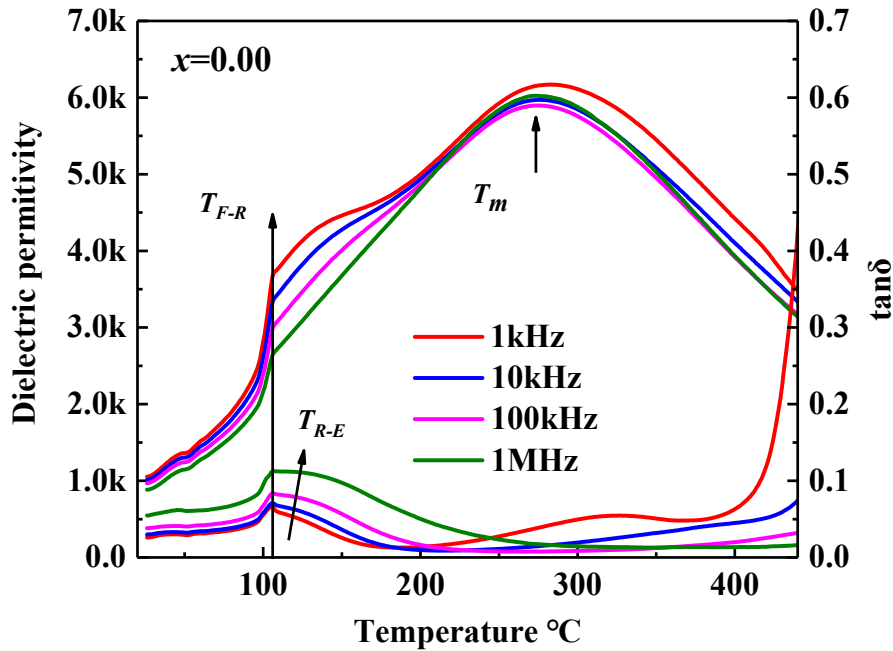


Fig. S3. Temperature-dependent dielectric responses of poled NBT-7BT sample.

Fig. S3 gives the temperature-variable dielectric responses of poled NBT-7BT sample, which is same as reported previously<sup>3</sup>. There are three dielectric anomalies in the temperature-variable dielectric responses of poled NBT-7BT sample: The first anomaly at 106 °C is independent of the frequency, which indicates the ferroelectric-relaxor transition, and is referred as to  $T_{F-R}$ . Upon temperature arising, strong frequency dispersion in  $\epsilon_r$  and  $\tan\delta$  was observed, and the frequency-dependent dielectric dispersion diminishes gradually; meanwhile, a frequency-dependent maximum of  $\tan\delta$  was observed around 150 °C in  $\tan\delta$ - $T$  curves, which is defined as  $T_{R-E}$ . Further increasing the temperature, a frequency-dependent maximum of the  $\epsilon_r$  was observed, which corresponds to the thermal relaxation of ergodic PNRs, and is defined as  $T_m$ .

## References:

1. Z. Zhu, L. Luo, F. Wang, P. Du, X. Zhou, Q. Zhang, W. Li and Y. Wang, *Journal of the European Ceramic Society*, 2020, **40**, 689-698.
2. J. Rödel, W. Jo, K. T. P. Seifert, E.-M. Anton, T. Granzow and D. Damjanovic, *Journal of the American Ceramic Society*, 2009, **92**, 1153-1177.
3. C. Ma and X. Tan, *Solid State Communications*, 2010, **150**, 1497-1500.